Characterization of the Flow (Breakup) Regimes in a Twin-Fluid Atomizer based on Nozzle Vibrations and Multivariate Analysis

Raghav Sikka[1] Maths Halstensen[2] Joachim Lundberg[1]

[1] Department of Process, Energy and Environmental Technology, University of South-Eastern Norway, Norway, Raghav.sikka@usn.no

[2] Department of Electrical Engineering, IT and Cybernetics, University of South-Eastern Norway, Norway, Maths.Halstensen@usn.no

Abstract

In the study, a new non-intrusive approach based on acoustic chemometrics, which includes vibration signal collection using glued-on accelerometers, was assessed for the classification of the different flow (breakup) regimes spanning a whole range of fluids (water and air) flow rates in this twin-fluid atomizer *(one-analyte system)*. This study aims to determine the flow regimes based on the dimensionless number (B), whose unique values correspond to different flow (breakup) regimes. The principal component analysis (PCA) was employed to visually classify the breakup regimes through cluster formation using score plots. The model prediction performance was studied using PLS-R, RMSEP values show error ranges within acceptable limit when tested on independent data. The present acoustic study can serve as a good alternative to the imaging methods employed for flow classification.

Keywords: Multivariate Regression, Acoustic Chemometrics, Principal Component Analysis, Flow Regimes

1 Introduction

Twin-fluid atomizers have been widely used atomizers in various applications such as the aerospace industry, internal combustion engines, process industry, spray drying, etc. Classification of the flow regimes using a high-speed imaging setup is quite common, as mentioned in different twin-fluid studies (Choi, 1997; Leboucher et al., 2010). While it is a fairly convenient way to categorize flow regimes for a laboratory-scale test setup using imaging setup (Adzic et al., 2001; Li et al., 1999), it can be a greater concern for industrial-scale atomizers due to the significantly larger fluid flow rates. Acoustic chemometrics, thoroughly applied (Esbensen et al., 1999; Halstensen et al., 2000) lately has proved to be a decent approach for tackling fluid-related problems. The applications for acoustic chemometrics are multitude, ranging from qualitative analysis to process monitoring. The ambit of acoustic analysis lies in the fact that all flow processes comprise some form of energy output emission in the form of signals that can be tapped and analyzed. The flow in the nozzles gives rise to certain vibrations for a particular set of fluid flow rates. By recording those signals through a data acquisition device using sensors (accelerometers) and performing signal analysis, useful qualitative information can be extracted by multivariate analysis.

To suffice the currently used imaging methods for flow regimes classification, an experimental setup, including novel twin-fluid atomizers, is investigated with real-time monitoring of the acoustic signal data. This study aims to assess the feasibility of the acoustic chemometrics approach for this air-assisted spray atomizer problem. The main objective is to determine the flow regimes based on the dimensionless number B, whose unique set of values corresponds to different flow (breakup) regimes. This analysis will further cater to whether the acoustics chemometrics approach, including both unsupervised learning technique (PCA) and supervised learning technique (PLS-R), is suitable for extracting valuable information through recorded vibration signals.

2 Materials and Methods

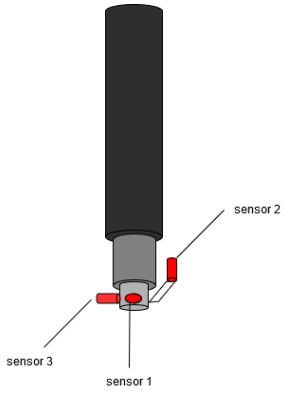

Figure 1. Schematic of the novel atomizer attached at the end of the lance, along with the accelerometers (in red).

2.1 Experimental Method

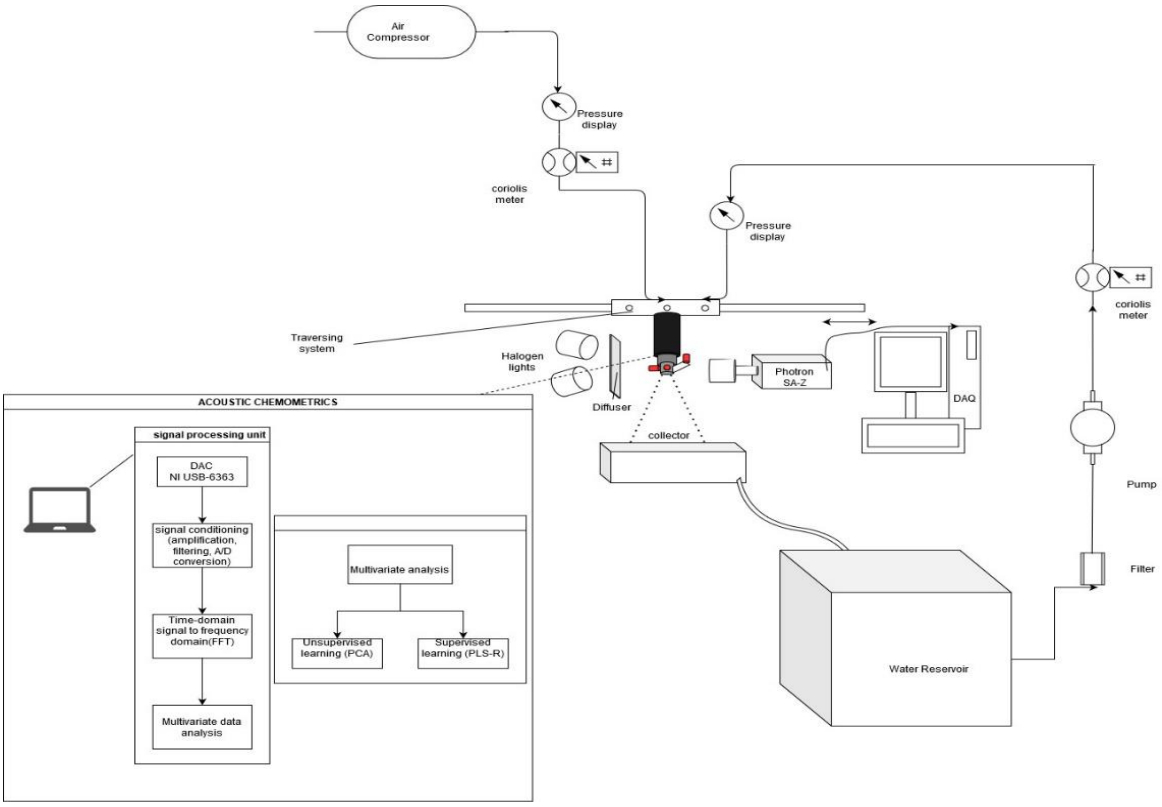

Figure 2. Schematic of the experimental setup along with the acoustic chemometrics flow chart (in box).

The experiments were carried out in a laboratory-scale experimental test rig in the process energy laboratory at the USN. The test rig consists of the lance, which is mounted at the traversing system, at whose end a twin-fluid atomizer (Figure 1) with 3.0 mm orifice (throat) diameter for core air was attached. The sensors in the three-axis (x, y, and z) were glued onto the atomizer. The liquid (water) was flowing in an annular manner through a slit of 280 µm along with the high-speed air core with the aid of hoses and pipes attached to the lance (Figure 2).

The high-speed imaging performed using the CMOS Photron camera SA-Z and two 250 W each Halogen lights from Dedocool Dedolight renders the different flow regimes visible at certain different fluid flow rates (Figure 3). Certain breakup regimes or modes were found at specific air-to-liquid mass ratios (ALR) and Weber number (We) based on liquid sheet velocity. ALR is defined as:

$$ALR = \frac{m_{air}}{m_{liquid}} \quad (1)$$

where mass flow rate in kg/hr.

Weber number is defined as:

$$We = \frac{\rho U^2 t}{\sigma} \quad (2)$$

Where ρ is liquid density (1000 kg/m^3), U is sheet velocity calculated through mass flow rate, σ is surface tension, and t is sheet thickness (280 µm).

A new dimensionless number (B) (depicted in Table 1) was employed, which is defined as:

$$B = We \cdot ALR \quad (3)$$

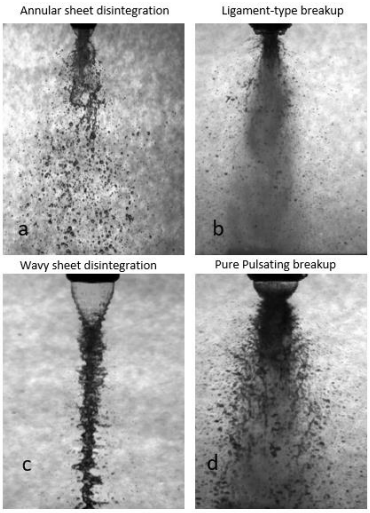

Figure 3. Different breakup regimes based on different fluid mass flow rates.

Table 1. Breakup regimes and the corresponding non-dimensional number values

Breakup Regimes	***B***	***ALR***	***We***
Annular sheet disintegration	2.586	0.150	17.24
Ligament type breakup	6.035	0.350	17.24
Wavy sheet breakup	9.052	0.0428	211.2
Pure-pulsating breakup	21.12	0.10	211.2

Both fluid flow rates were measured and monitored using Coriolis flowmeters. Two air flow rates (15 kg/hr and 35 kg/hr) were employed as per the visualization study and manually operated through the pressure regulator. 100 kg/hr corresponds to Weber number (We) of 17.24, whereas 350 kg/hr corresponds to Weber number (We) value of 211.2. The liquid (water) flow rates taken were low flow rate (100 kg/hr) and high flow rate (350 kg/hr), which were altered through a frequency-based flow rate controller. The air-to-liquid ratio varied from 0.0428 to 0.35, depending on the combination of fluid flow rates as depicted in Table 1. At lower flow rates, annular sheet disintegration was visualized, whereas it reached pure-pulsating breakup mode at higher flow rates for both air and water. Ligament type breakup corresponds to high airflow rates & low liquid flow rates, whereas wavy sheet breakup corresponds to high airflow rates & low liquid flow rates, as mentioned in Figure 3.

2.2 Acoustic chemometrics

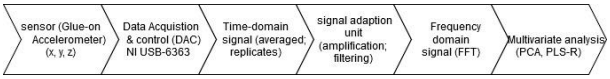

Figure 4. Block diagram of the acoustic analysis in-flow process from the vibration data collection.

The name acoustic chemometrics (Esbensen et al., 1998) implies that the information extraction from the data recorded in vibrational energy is measured using some acoustic sensors (say, accelerometers). Some inherent advantages related to acoustic chemometrics are:

- Non-intrusive technology system
- Real-time monitoring of signals
- Easy sensor deployment (glued-on)
- Relatively inexpensive technology
- Prediction of several parameters from the same acoustic spectrum

The acoustic measurements in this study were taken using sensors (accelerometer, which is a piezoelectric type 4518) from Bruel & Kjær, Denmark. Three sensors are utilized in the test experiments to tap the noise/vibration data from all three axes (x, y, and z), as depicted in Figure 1. The fluid flow ejected out of the atomizer outlet forces the atomizer a sudden backward blow, recorded in an electrical signal proportional to the vibration acceleration. A signal amplification unit, a data acquisition device (NI USB-6363) from National Instruments and a personal laptop were employed. NI USB-6363 data acquisition device (DAQ) was utilized to acquire the signal, where the signal converted from analog to digital. A digital signal is required for the signal amplification unit for further processing. The frequency range used for this study is (0 - 200 kHz).

For the acoustic chemometrics signal collection and signal conditioning, the LabVIEW-based in-house created interface (Halstensen et al., 2019) was used. The signal processing was carried out in few steps. Firstly, time series of 4096 samples were recorded from the sensor. The time-series signal was multiplied by a window (Blackman Harris), which cancels the end of the series to avoid spectral leakage in the acoustic spectrum. This signal is finally transformed into the frequency domain using Discrete Fourier Transform (DFT). The Discrete Fourier Transform transforms a sequence of N complex numbers $\{x_n\}:= x_0,x_1,...,x_{n-1}$ into another sequence of complex numbers, $\{X_k\}:= X_0,X_1,...,X_{N-1}$, which is defined by equation:

$$X_k = \sum_{n=0}^{n-1} x_n \, e^{-i2\pi kn/N} \;\; k = 0, \dots, N-1 \qquad (4)$$

A more advanced and efficient form of the DFT is the Fast Fourier Transform (FFT) (Ifeachor et al., 1993), which was implemented in the LabVIEW interface for fast real-time calculation. The whole in-flow acoustic analysis process from signal conditioning to domain transformation from time to frequency and then supervised (PLS-R) and unsupervised (PCA) multivariate analysis techniques are mentioned in a block diagram (Figure 4).

2.3 Principal Component Analysis (PCA)

Principal component analysis (PCA) analyses multivariate data by examining the common variances. Large multivariate data sets can be noisy and difficult to interpret. PCA projects mean-centred data (X) consisting of variables (columns) and samples (rows) onto a new plane. The new plane is represented by scores (T) and loadings (P). E is the notation of the data not explained by the model, the residuals, given by the equation:

$$X = T\,P^T + E \tag{5}$$

PCA uses an orthogonal transformation to convert correlated variables into few linearly uncorrelated variables called principal components. The method is called the unsupervised method due to no guidance to the singular value decomposition from the data. The nonlinear Iterative Partial Least Squares (NIPALS) algorithm developed earlier (Wold et al., 1987) was used because of its many advantages. It works on matrices with moderate amounts of randomly distributed missing observations. The other advantage of NIPALS is that it is less time-consuming than Singular value decomposition (SVD), as the former allows defining the number of components to calculate.

2.4 Partial Least Squares Regression

Partial least squares regression (PLS-R) is a supervised method used for calibrating the predicting models, which is well explained in (Geladi et al., 1986).

PLS-R is a good alternative to other regression techniques due to its robustness. The model parameters do not change much even when new calibration samples are taken from the population. It relies on representing training data for two-variable blocks X and Y, respectively. In the present work, the X data matrix contains the acoustic frequency spectra, and Y is a vector containing the non-dimensional number B values that define the breakup regimes.

The NIPALS algorithm is the most widely used in the PLS regression technique. In this algorithm, PLS-R allows modelling both the X and Y simultaneously, which might raise orthogonality issues. For low precision data, PLS-R gives more accurate results than other regression methods. A simplified version of the NIPALS algorithm is presented in earlier studies (Ergon et al., 2001), where A is an optimal number of components. A step-wise NIPALS algorithm is described in some detail (Halstensen, 2020).

In evaluating the regression model, the root mean squared error of prediction RMSEP offset, slope and correlation coefficient are commonly used. Besides these, visual evaluation of the relevant T-U score plots, loading weights plots, explained variance plots also provide useful information for calibrating and developing the prediction model. The root mean square is given by:

$$\text{RMSEP} = \frac{\sqrt{\Sigma_{i=1}^{n}\left(\hat{y}_{i,predicted} - y_{i,reference}\right)^2}}{n} \tag{6}$$

Where, i = sample index number
n = total number of samples
RMSEP = Root Mean Squared Error of Prediction.

3 Results and Discussion

3.1 PCA results

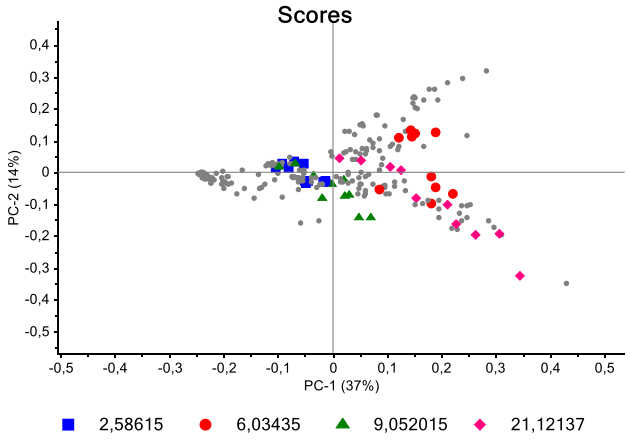

Figure 5. Score plot t1-t2 for both atomizer.

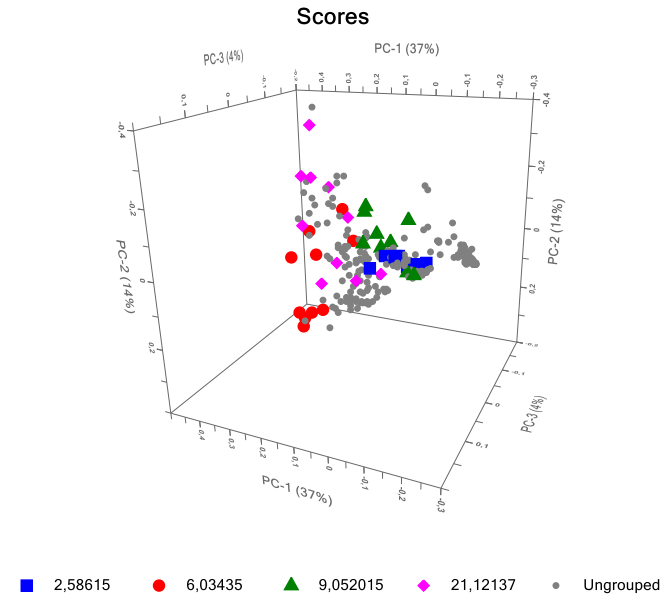

Figure 6. 3-D Score plot t1-t2 for both atomizers.

PCA score-plots depicts how the acoustic spectrum and different breakup regimes are correlated based on the tests carried out at various flow rates. A colour indicates each breakup regime in the data-centred score plot. The score plots show a cluster of points for a particular type of breakup regime/mode for principal component 1. The score plot shows a trend in the data from low airflow rates on the left side (blue) to the high air flow rates on the right side (pink).

The score plots were obtained with the whole frequency spectrum for all three sensors deployed. The score plots depicting two different atomizer type-converging and converging-diverging (CD) atomizer. To avoid repeatability, both converging and converging-diverging (CD) atomizer are shown in a single score plot as a 2-D plot (Figure 5) and for better visualization as in a 3-D plot (Figure 6). The loading plot (Figure 7) shows that the information based on the frequencies recorded from sensor 2 is different from the other two sensors, provided that sensor 2 is located opposite to the fluid flow direction, which is relevant in this case.

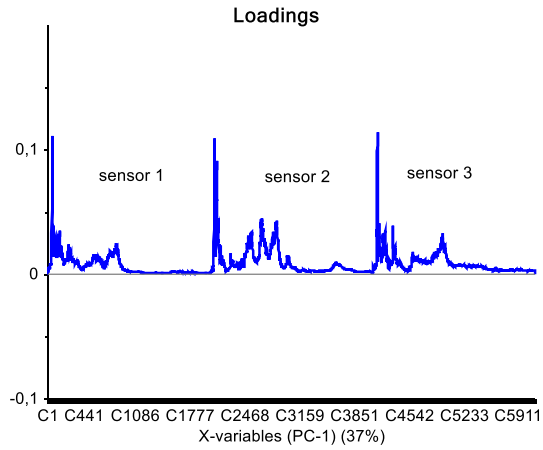

Figure 7. Loadings plot for all three sensors.

3.2 PLS-R prediction for the breakup regimes

PLS-R was employed to do model prediction based on the acquired acoustic spectra. The non-dimensional number (B) values were used as the reference values (Figure 8). The acoustic spectra used to calibrate the PLS-R model was a 240x2048 matrix containing 240 frequency spectra for each sensor. The test set validation was performed for alternate data matrix values, 50 % (120) of the total column set. Each spectrum consisted of 2048 frequencies ranging from 0 to 200 kHz. The statistical parameters that evaluate the model prediction are slope and RMSEP. Both slope and RMSEP define the model's quality fitting the reference data; in this case, their value is reasonably within permissible limits.

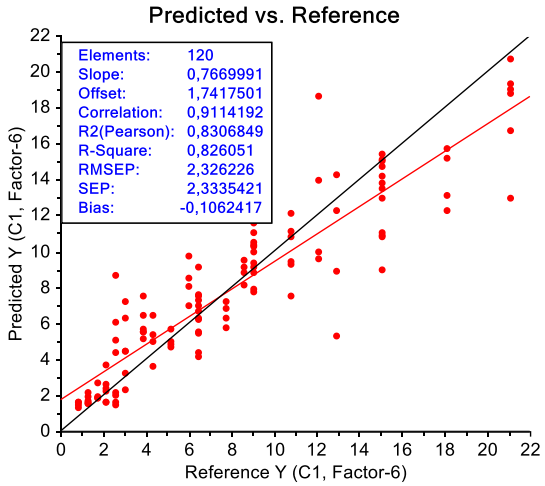

Figure 8. Predicted Vs. Reference (B) value. The target line (black) and regression line (red) are indicated.

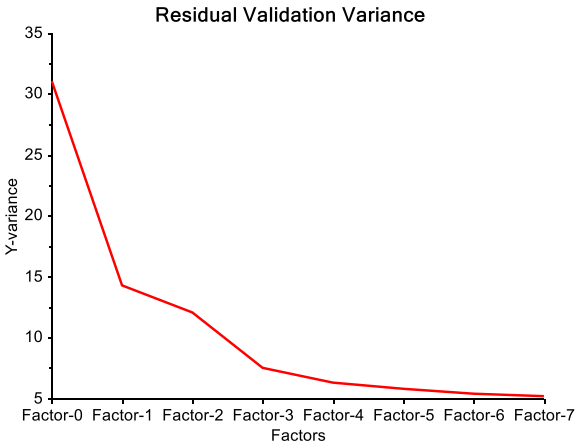

Figure 9. Residual validation variance plot.

Based on the residual validation variance plot (Figure 9), six components can be fixed as optimal for model prediction. The same results can be plotted as samples taken in time (Figure 10). The green line is the reference line for non-dimensional number (B), and the blue line is the prediction line.

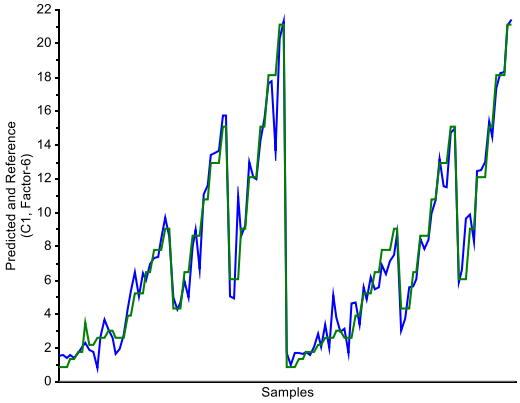

Figure 10. Predicted and Reference (B) values for samples taken in time.

4 Conclusions

To corroborate the visualization study performed for breakup regimes identification, the non-invasive acoustic/vibrations study incorporating sensors (accelerometer) with an appropriate signal processing system was performed, allowing the estimation of the flow breakup modes. The feasibility of this approach for fluid flow classification is the main objective of this study, rendering relevant information about the flow breakup regimes for various fluid flow rates. The acoustic measurements provide valuable insight into the regime classification based on a derived dimensionless number (B) from other fluid-based non-dimensional numbers. The pattern study using principal component analysis provides relevant information through the clusters formed for each breakup regime. The chemometric method provided sufficiently good model prediction with slope and RMSEP values within acceptability limits. The main advantage of this non-invasive acoustic method is that it renders the visualization study for different breakup modes optional for industrial-scale atomizers for flow regime prediction which can be implemented on the industrial-scale setup.

References

M. Adzic, I. S.Carvalho, and M. V. Heitor. Visualization of the disintegration of an annular liquid sheet in a coaxial air-blast injector at low atomizing air velocities. *Optical Diagnostics in Engineering*, *5*(1), 27–38, 2001.

C. J. Choi. Disintegration of Annular Liquid Sheet with Core Air Flow -Mode Classification. *International Journal of Fluid Mechanics Research*, *24*(1–3), 399–406, 1997.

R. Ergon, and K. H. Esbensen. A didactically motivated PLS prediction algorithm. *Modeling, Identification and Control*, *22*(3), 131–139, 2001. doi: 10.4173/mic.2001.3.1

K. H. Esbensen, M. Halstensen, T. Tønnesen Lied, Saudland Arild, J. Svalestuen, S. De Silva and Hope, B. Acoustic chemometrics - From noise to information. *Chemometrics and Intelligent Laboratory Systems*, *44*(1–2), 61–76, 1998. doi: 10.1016/S0169-7439(98)00114-2

K. H. Esbensen, B. Hope, T. T. Lied, M. Halstensen, T. Gravermoen and K. Sundberg. Acoustic chemometrics for fluid flow quantifications - II: A small constriction will go a long way. *Journal of Chemometrics*, *13*(3–4), 209–236, 1999. doi: 10.1002/(sici)1099-128x(199905/08)13:3/4<209::aid-cem553>3.0.co;2-5

P.Geladi, and B. R. Kowalski. PARTIAL LEAST-SQUARES REGRESSION: A TUTORIAL. *Analytica Chimica Acta*, *185*, 1–17, 1986.

M. Halstensen. *Classification of Gases and Estimation of Gas Flow Rate Based on Unsupervised and Supervised Learning Respectively*.*September*,22–24,2020. doi: 10.3384/ecp20176451

M. Halstensen and K. Esbensen. New developments in acoustic chemometric prediction of particle size distribution - "The problem is the solution." *Journal of Chemometrics*, *14*(5–6), 463–481, 2000. doi: 10.1002/1099-128X(200009/12)14:5/6<463::AID-CEM628>3.0.CO;2-Y

M. Halstensen, J. Lundberg, P. I. Januschas and H. P. Halvorsen. On-line Monitoring of Viscous Properties of Anti-icing Fluid Based. *Proceedings of The 60th SIMS Conference on Simulation and Modelling SIMS 2019, August 12-16, Västerås, Sweden*, *170*, 26–31, 2019. doi: 10.3384/ecp2017026

E. C. Ifeachor and B. W. Jervis,. *Digital signal Processing*, 1993.

N. Leboucher, F. Roger and J. L. Carreau. Disintegration process of an annular liquid sheet assisted by coaxial gaseous coflow(S). In *Atomization and Sprays* (Vol. 20, Issue10,847–862,2010. doi:10.1615/AtomizSpr.v20.i10.20

X. Li and J. Shen. Experimental study of sprays from annular liquid jet breakup. *Journal of Propulsion and Power*, *15*(1), 103–110, 1999. doi: 10.2514/2.5397

S. Wold, K. Esbensen and P. Geladi. Principal Component Analysis. *Chemometrics and Intelligent Laboratory Systems*,*2*(1–3),37–52,1987. http://files.isec.pt/DOCUMENTOS/SERVICOS/BIBLIO/ Documentos de acesso remoto/Principal components analysis.pdf